Journal of Colloid and Interface Science **243,** 370–381 (2001)
doi:10.1006/jcis.2001.7881, available online at http://www.idealibrary.com on IDEAL®

Mixed Langmuir Monolayer of *N*-(1,1-Dihydroperfluorododecyl)-*N*,*N*,*N*-Trimethylammonium Chloride with Perfluorocarboxylic Acids

Muhammad Rusdi,* Yoshikiyo Moroi,*,[1] Shohei Nakamura,† Osamu Shibata,†,[1] Yutaka Abe,‡ and Toshio Takahashi‡

*Department of Chemistry and Physics of Condensed Matter, Graduate School of Sciences, Kyushu University-Ropponmatsu, 4-2-1 Ropponmatsu, Chuo-ku, Fukuoka 810-8560, Japan; †Department of Molecular Bioformatics, Graduate School of Pharmaceutical Sciences, Kyushu University, 3-1-1 Maidashi, Higashi-ku, Fukuoka 812-8582, Japan; and ‡Material Science Research Center, Lion Corporation, 7-13-12 Hirai, Edogawa-ku, Tokyo 132-0035, Japan

Received December 12, 2000; accepted July 27, 2001; published online October 5, 2001

Surface pressure (π)–area (A), surface potential (ΔV)–area (A), and dipole moment ($\mu_\perp$)–area (A) isotherms for *N*-(1,1-dihydroperfluorododecyl)-*N*,*N*,*N*-trimethylammonium chloride (C12-TAC) and perfluorododecanoic acid (FC12) on the substrate of 0.01 M sodium chloride at pH 2.0 were investigated at the air–water interface by the Langmuir method and the ionizing electrode method. The temperature dependence of the transition pressure of each component was not larger than that of normal hydrogenated surfactant. The apparent molar entropy, enthalpy, and internal energy changes of phase transition from the disordered to the ordered state were calculated. Surface potentials (ΔV) were analyzed using the three-layer model proposed by R. J. Demchak and T. Fort (*J. Colloid Interface Sci.* 46, 191–202, 1974) for FC12 and Gouy–Chapman treatment for C12-TAC. The contributions of the ω-CF_3 group and the head group of the vertical component to the dipole moment, $\mu_\perp$, were estimated. The new finding was that the π–A curves are shifted to an area smaller than a molecular area of two pure components for the mole fraction (x) of perfluorododecanoic acid of $x \geq 0.3$. The molecular areas negatively deviate from the additivity rule at discrete surface pressures. Assuming a regular surface mixture, the Joos equation (Joos, P., and R. A. Demel, *Biochim. Biophys. Acta* 183, 447, 1969) for analysis of the collapse pressure of mixed monolayer allowed estimation of the interaction parameter; $\xi = -4.20$ at $x \leq 0.5$ and $\xi = -0.24$ at $x > 0.5$ between two fluorinated amphiphiles. © 2001 Academic Press

Key Words: **Langmuir monolayers; fluorinated surfactants; surface potentials; dipole moments; two-dimensional phase diagram; π–A isotherm; ΔV–A isotherm.**

INTRODUCTION

Fluorinated amphiphiles or surfactants are characterized by stronger surface activity at an interface and by enhancing properties to aggregate at concentrations lower than those of their corresponding hydrogenated amphiphiles (1). This is because a fluorine atom is the most electronegative of all elements. A perfluorocarbon chain has very strong intramolecular chemical bonds but very weak intermolecular interaction at the same time. Therefore, it is no wonder that fluorocarbon chains have very interesting behaviors that are quite different from those of hydrocarbon chains. Many kinds of new, well-defined, and modular fluorinated amphiphiles were recently synthesized, which allowed formations of various stable colloidal systems with potential biomedical applications (2). The colloidal systems include fluorocarbon-in-water emulsion, reverse water (or hydrocarbon)-in-fluorocarbon-in-water emulsion (3), and microemulsion, fluorinated vesicles (4), and fluorinated microtubules (5). In addition, fluorocarbons are efficient oxygen carriers (6).

Various kinds of mixed monolayers made from hydrogenated surfactant spread at the air/water interface have been studied (7–10). However, reports on fluorinated surfactants are still much fewer in number than reports on hydrogenated surfactants. In previous studies, one of the authors has investigated a mixed monolayer system of dipalmitoylphosphatidylcholine (DPPC) and hydrogenated or perfluorocarboxylic acids (11, 12) and reported that perfluorocarboxylic acids and DPPC are partially miscible in the mixed monolayers. The intermolecular interaction was rather strong, suggesting that attractive force between the two head groups contributes more to miscibility than hydrophobic interactions between long alkyl chains (11). As for monolayer made from DPPC or dipalmitoylphosphatidylethanolamine (DPPE) and semifluorinated alkanes, on the other hand, the semifluorinated alkanes were ejected out from the water surface at higher surface pressure and reversibly formed a second organized layer above a phospholipid-only monolayer (13, 14).

In the present study, the authors have investigated the monolayer behavior of *N*-(1,1-dihydroperfluorododecyl)-*N*,*N*,*N*-trimethylammonium chloride (C12-TAC) and perfluorododecanoic acid (FC12) and of their mixtures at the air/subsolution interface. The C12-TAC is a newly synthesized cationic fluorinated amphiphile and, therefore, has never been studied from

[1] To whom correspondence should be addressed. E-mail: moroiscc@mbox.nc.kyushu-u.ac.jp. E-mail: shibata@mail.phar.kyushu-u.ac.jp.

0021-9797/01 $35.00

the point of Langmuir monolayer (15). The characteristic of the molecule is that the shape is rod-like from tail to head with the same diameter or of the packing parameter one. First of all, surface pressure (π)–, surface potential (ΔV)–, and dipole moment ($\mu_\perp$)–area (A) isotherms were obtained for the pure compounds and their mixtures. Second, surface potentials were analyzed using the three-layer model proposed by Demchak and Fort (16) and the surface potential obtained with the Gouy–Chapman equation. Third, the phase behavior of the mixed monolayers was examined in terms of the additivity of molecular surface area, surface potential, and surface dipole moment and by using the Joos equation (17) for the molecular interaction.

EXPERIMENTAL

FC12 and perfluorodecanoic acid (FC10) were purchased from Fluorochem (United Kingdom). They were purified by repeated recrystalizations from *n*-hexane/acetone mixed solvent (11 : 1, v/v). The purity of these surfactants was checked by ^{19}F NMR measurement (UNITY INOVA 400 Spectrometer, Varian, USA) and by elemental analysis; the observed and calculated values were in satisfactory agreement ($<\pm 0.3\%$). *N*-(1,1-dihydroperfluorododecyl)-*N*,*N*,*N*-trimethylammonium chloride was synthesized as reported previously (15). The pure compounds or their mixtures were spread from the *n*-hexane/ethanol mixture (7/3) at the air/aqueous solution interface. *n*-Hexane and ethanol came from Merck (Uvasol) and Nacalai Tesque, respectively.

The 0.01 M (1 M = 1 mol dm^{-3}) sodium chloride (Nacalai Tesque) substrate solution was prepared using thrice distilled water (surface tension, 72.7 mN m^{-1} at 293.2 K; resistivity, 18 MΩ) the pH of which was maintained at 2 by hydrochloric acid (ultra fine grade; Nacalai Tesque). Sodium chloride was roasted at 700 K for 24 h to remove any surface active organic impurity.

The surface pressure of the monolayer π was measured using an automated Langmuir film balance, which was the same used in the previous studies (18). The surface pressure balance (Chan RG, Langmuir float type) had a resolution of 0.01 mN m^{-1}. The trough was made from a 750-cm^2 brass sheet coated with Teflon. The monolayer was compressed at a speed of 2.00×10^{-1} nm^2 molecule^{-1} min^{-1}. No influence of the compression rates (at 6.60×10^{-2}, 1.00×10^{-1}, and 2.00×10^{-1} nm^2 molecule^{-1} min^{-1}) was detected within the limits of the experimental error. Surface potential was simultaneously recorded while the monolayer was compressed. It was monitored using an ionizing ^{241}Am electrode at 1–2 mm above the interface, while a reference electrode was dipped in the subphase. The standard deviation for the area was approximately 1.00×10^{-2} nm^2, while that for surface potential was 10 mV. Fluorescence microscopy (U.S.I. System BM-1000) observation was carried out; 3,6-bis(diethylamino)-9-(2-octadecyloxycarbonyl)phenyl chloride (R18 : Molecular Probes) was used as the fluorescence probe. A spreading solution of surfactants was prepared in *n*-hexane : ethanol (7 : 3, v/v), and the probe concentration was $(7.9–8.0) \times 10^{14}$ molecules/μl with 1 mol% fluorescence probe. Other experimental conditions were the same as those described in the previous papers (18).

RESULTS AND DISCUSSION

1. *Surface Pressure (π)–, Surface Potential (ΔV)–, and Dipole Moment ($\mu_\perp$)–Area (A) Isotherms*

FC12 and C12-TAC did not form a stable monolayer on pure water, and, therefore, the substrate condition was examined at the first step. The optimum pH of the substrate was found to be 2 under the condition of 0.01 M NaCl (1 M = 1 mol dm^{-3}). This condition was maintained throughout the experiments.

The π–A, ΔV–A, and $\mu_\perp$–A isotherms of monolayers made from pure FC12 and C12-TAC spread on the above subsolution at 298.2 K are shown in the (Figs. 1a–1b). The π–A, ΔV–A, and $\mu_\perp$–A isotherms of the FC12 monolayer at the surface (Figs. 1a and 1b) are very close to those previosly reported (12) except for minor distinctions caused by dissimilarities in the

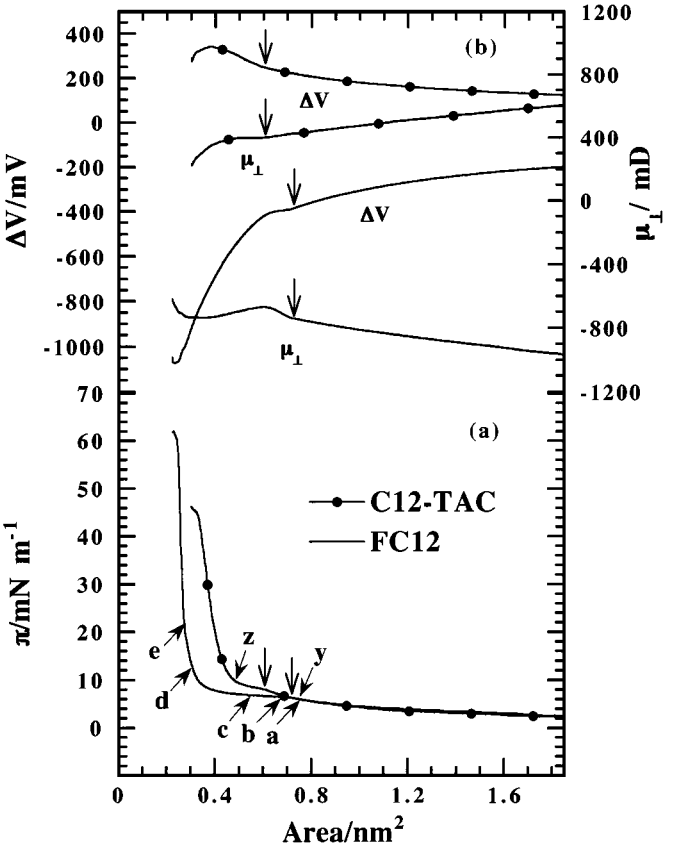

FIG. 1. Surface pressure (π)–area (A) isotherms (a), surface potential (ΔV)–A isotherms (b), and surface dipole moment ($\mu_\perp$)–A isotherms (b) of FC12 and C12-TAC on 0.01 M NaCl (pH 2) at 298.2 K. Designated arrows of FC12 (a, b, c, d, e) and C12-TAC (y, z) correspond to the fluorescence micrograph images in Fig. 3.

subphase composition. The vertical component of the surface dipole moment, $\mu_\perp$, was calculated from the Helmholtz equation:

$$\Delta V = \mu_\perp/\varepsilon_0\varepsilon A, \qquad [1]$$

where ε_0 is the permittivity of the vacuum and ε the mean permittivity of the monolayer (which is assumed to be one). FC12 was stable up to 60 mN m^{-1} with a transition from a disordered phase (gaseous or expanded) to an ordered (LS) one at 6.2 mN m^{-1} (0.73 nm^2) as indicated by an arrow (Fig. 1a). The extrapolated area in the condensed state was 0.28 nm^2 and the collapsed area 0.24 nm^2. These values indicate that the fluorinated chains are in close contact at high pressure. The C12-TAC isotherm was more expanded with a transition from one phase to the other phase at 8.2 mN m^{-1} (0.62 nm^2) as indicated by an arrow (Fig. 1a). It collapsed at 44 mN m^{-1} (0.33 nm^2) with an extrapolated area of 0.45 nm^2. To check the stability of the monolayer, the relaxation of surface pressure for stearic acid, FC12, C12-TAC, and a 1 : 1 mixture of FC12 and C12-TAC after compression up to 35 mN m^{-1} was measured under the above subphase condition. Figure 2 shows that the surface pressure of FC12 and C12-TAC decreases more slowly than that of stearic acid. Therefore, the former two monolayers are more stable than the latter. In addition, the increase of the surface pressure exhibited by the 1 : 1 mixture of FC12 and C12-TAC supports a complex formation between them as discussed latter.

Figure 3 independently proves the appearance of a condensed phase in the FC12 film between 0.74 and 0.69 nm^2, and the coexistence of condensed and disordered phases continues down to 0.31 nm^2. The present fluorescence microscopy confirms the coexistence of two phases, as is shown by the plateau in the π–A isotherm in Fig. 1a. The order phase is an LS phase, because a direct *in situ* investigation of the same monolayer via grazing incidence X-ray diffraction shows a single resolution-limited first-order peak at 1.25 Å^{-1} and a second-order peak at 2.16 Å^{-1} (19). Such a picture is typical of a hexagonal lattice of closely packed upright molecules. At 4°C the resolution-limited peak was observed from 5 nm^2 down to 0.3 nm^2. This fact shows the coexistence of an ordered phase and a gaseous phase. However, at 20°C the resolution-limited peak of the ordered phase was not found above 0.80 nm^2, which is in excellent agreement with the above fluorescent microscopy data (Fig. 3) and with the isotherm in Fig. 1a. The structure found by the experimental study has also been confirmed via molecular dynamic simulation of the $CF_3(CF_2)_{13}COOH$ monolayer at 8 mN/m and 300 K by Shin and Rice (20). Another theoretical paper by same authors (21) explains the presence and the absence of tilting transition in monolayers for hydrocarbon and perfluorinated or nearly perfluorinated amphiphiles, respectively, via different amphiphile–amphiphile and amphiphile–water interactions at the surface. All the above investigations show that a first-order phase transition indeed exists in the uncharged perfluorinated monolayer, but it does occur between a disordered phase (gaseous or expanded) and an ordered (LS) one. So, in this FC12 too, the first-order transition is from L2 to LS.

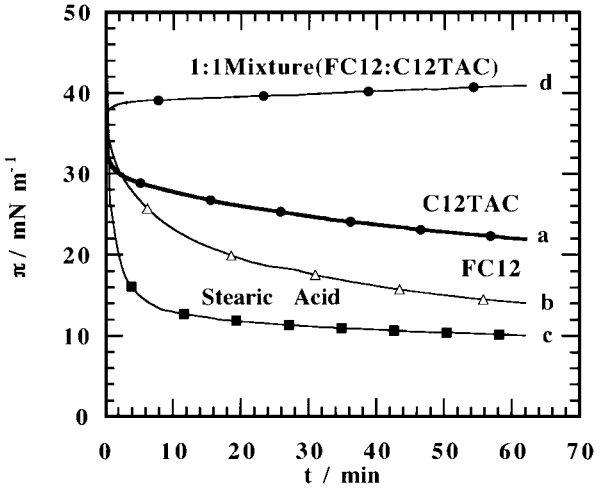

FIG. 2. Change in surface pressure with time. Langmuir monolayers were compressed up to 35 mN m^{-1} on 0.01 M NaCl (pH 2). Then, the π–t measurement was started. (a) C12-TAC, (b) FC12, (c) stearic acid, (d) 1 : 1 mixture (FC12 : C12TAC).

The surface potential measurement also clarifies the above phase transitions. The change in inclination of the ΔV (or $\mu_\perp$)–A isotherms vs molecular area curves corresponds to the transition pressure in the π–A isotherms. In the case where an inflection point appears in the ΔV–A or $\mu_\perp$–A isotherm, the points are indicated by an arrow (Figs. 1a and 1b). The surface potential (ΔV) of FC12 always showed a large negative variation of ΔV under compression (Fig. 1b). The ΔV value monotonously decreased and reached the value of -1070 mV starting from -200 mV with an absolute difference of 870 mV at the collapse pressure area (0.24 nm^2). On the other hand, the C12-TAC monolayer displayed a much smaller positive variation of ΔV from 100 to 350 mV near the collapse area. It has been shown that the surface potentials of monolayers of a series of ω-monohalogenated fatty acids and alcohols and of progressively fluorinated fatty acids were found negative due to the strong electronegativity of halogen atoms, while it was positive for the unsubstituted acids or alcohols (22–24). It was also found that ΔV did not change much with the number of carbon atoms in the fluorinated chain in the above studies (24), where the carbon atoms are more than 16 in number. In this study, however, the carbon number of the perfluoro chain is 12. The ΔV values involve the resultant of the dipole moments carried by the polar head (–COOH, or $-N^+(Me)_3\ Cl^-$), the C–F bond (the ω- CF_3 group), the subphase, and the change in the hydration of the polar head group. As the subphase and the hydrophobic tail of perfluoro chain are identical for the two compounds, the big difference in ΔV between FC12 and C12-TAC should originate from the neutral head group and the positive head group of the former and the latter, respectively.

The variation of the vertical component of the surface dipole moment $\mu_\perp$ of FC12 and C12-TAC monolayers under compression is also shown in Fig. 1b. A $\mu_\perp$ value strongly depends

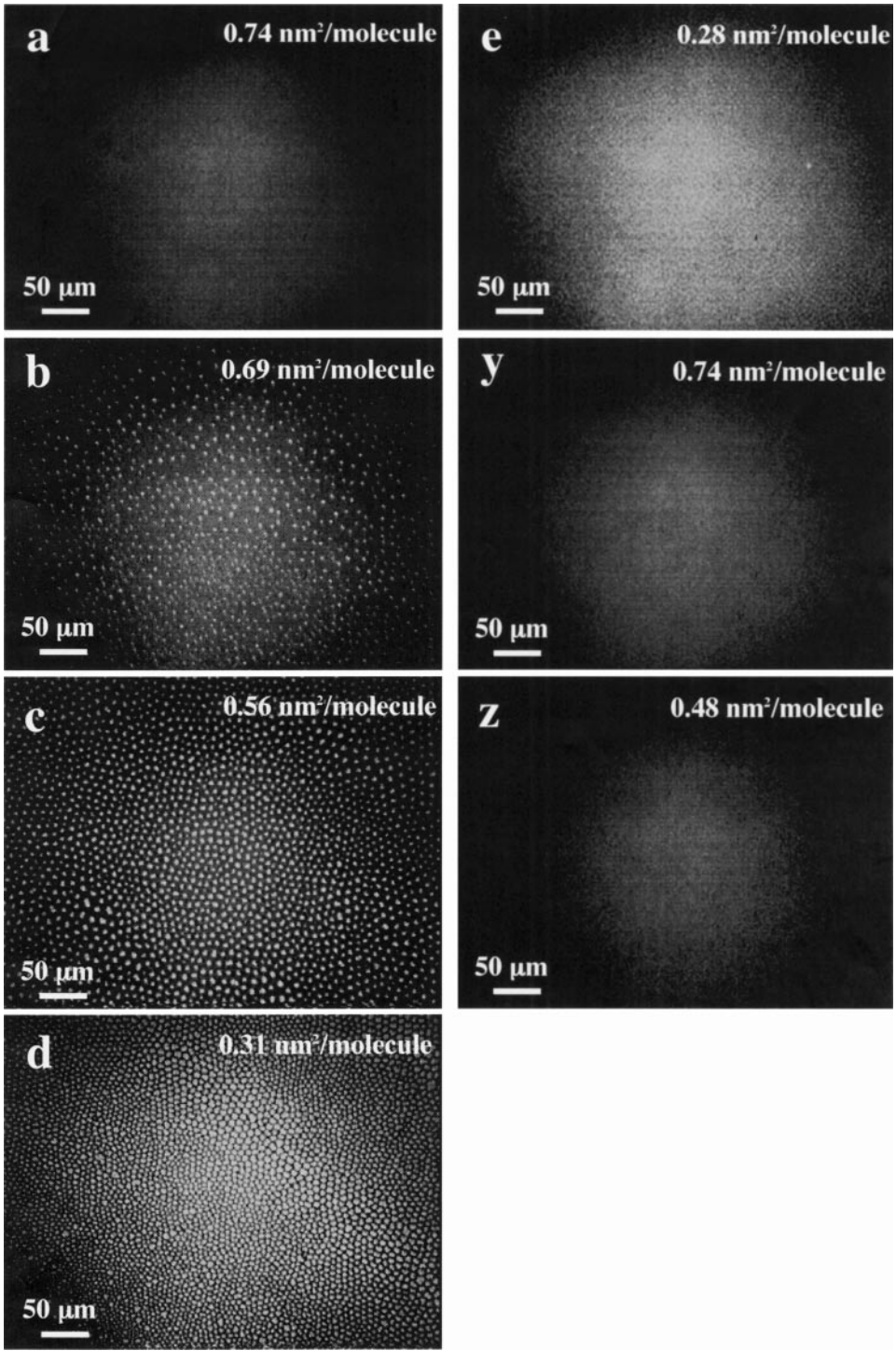

FIG. 3. Fluorescence micrographs of FC12 (a, b, c, d, e) and C12-TAC (y, z) observed at a continuous compression rate of 0.035 molecule^{-1} min^{-1} at 298.2 K on 0.01 M NaCl (pH 2). The monolayer contains 1 mol% fluorescent probe. The scale bar in the lower left represents 50 μm.

on the polar head group's nature. Upon compression, the $\mu_\perp$ (FC12) changed from -980 to -720 mD via a small hump, while $\mu_\perp$ (C12-TAC) monotonously decreased from 500 to 200 mD. Figure 1b displays the variation of $\mu_\perp$ over the area for the FC12 monolayer under compression from 1.85 to 0.20 nm^2. The $\mu_\perp$–A isotherm of FC12 did not reach a limiting plateau value as was usually observed (16, 24) but passed reproducibly through a minimum (-0.78 D) at 0.28 nm^2. This suggests that a

conformational change occurred in the monolayer, although the nature of this conformational change cannot be specified. A similar decrease of $\mu_\perp$ from 0.250 D at 0.222 nm^2 to 0.240 D at 0.200 nm^2 was also observed for the eicosanol monolayer (8). An unmonotonous variation of $\mu_\perp$ was reported for octadecyl nitrile (16), *n*-heptadecanol, and 16-bromohexadecanol monolayer, too (25). In the case of C12-TAC, it could not be ascertained that the variation of $\mu_\perp$ is monotonous, because the ΔV variation was small and because the change occurred near the collapse of the monolayers.

2. Apparent Molar Quantity Changes on the Phase Transition

The temperature effect on the transition pressure of the monolayers is of much interest, since it provides us with the thermodynamic information on the phase transition of monolayers. Figures 4a and 4b show the π–A isotherms of C12-TAC and FC12 at different temperatures, respectively. All the curves have a break point, showing the phase transition from L2 phase to an ordered (LS) one on compression. This phase transition was also confirmed by fluorescence microscopy (Fig. 3). As was expected, the transition pressures increased with increasing temperature. But the expansion in the π–A isotherms on transition is not so wide as that of the conventional surfactants composed of cationic hydrocarbon and anionic hydrocarbon as counterion (26, 27). In addition, temperature dependence of transition pressure is relatively small for FC12, while a larger temperature dependence is observed in the π–A isotherms of C12-TAC.

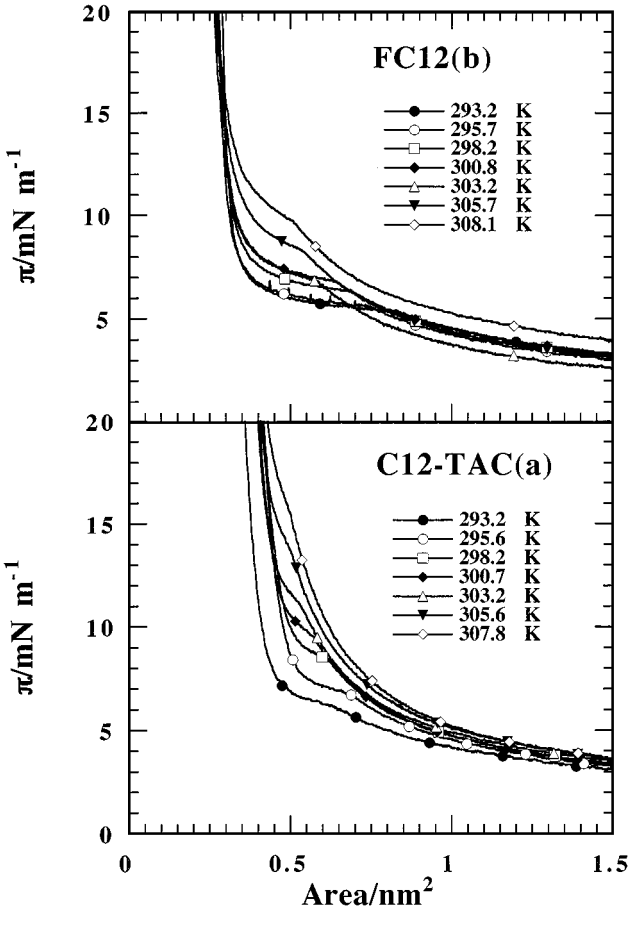

FIG. 4. Temperature dependence of surface pressure (π)–area (A) isotherms of FC12 and C12-TAC on 0.01 M NaCl (pH 2).

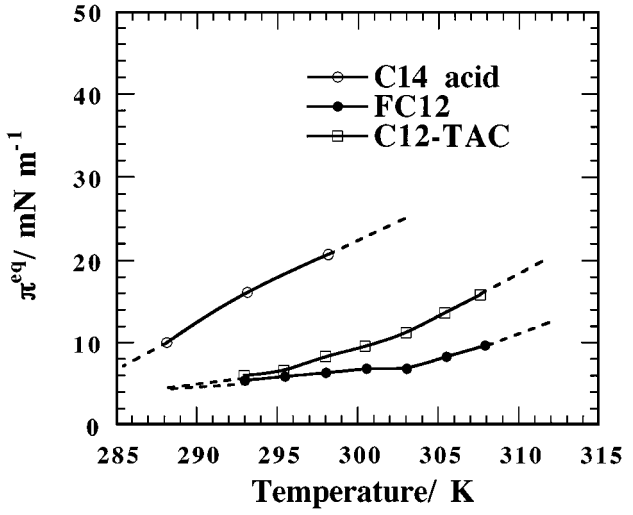

FIG. 5. Transition pressure (π^{eq}) as a function of temperature on 0.01 M NaCl (pH 2). C14 acid, tetradecanoic acid.

In Fig. 5, the transition pressure (π^{eq}) is shown as a function of temperature for perfluorinated amphiphiles. The curves are almost linear, and this figure also includes the temperature dependence of π^{eq} of tetradecanoic acid (C14 acid) in order to compare with that of perfluorinated amphiphiles. The slopes of these curves were used in order to calculate the apparent molar quantity change on the phase transition. The thermodynamic quantities on the phase transitions of monolayers were calculated by the previous method (18), which takes the contribution of the substrate of a monolayer into account. The apparent molar entropy change (Δs^γ) on the phase transition was evaluated by employing Eq. 29 of Ref. 28.

$$\Delta s^\gamma(\alpha, \beta) = (a^\beta - a^\alpha)[(\partial\pi^{eq}/\partial T)_p - (\partial\gamma^0/\partial T)_p] \quad [2]$$

In this equation, Δs^γ is an apparent molar entropy change, a^β and a^α are molecular areas (in square nanometers, the superscripts β and α refer phase states), π^{eq} is the transition pressure from the α phase to the β phase, and γ^0 is the surface tension of the substrate (29). a^β and a^α are estimated as follows. a^α is the area at the point where the film starts to transform from the α to the β state. The a^β value is determined in the following manner; when the point (π^{eq}, a^α) is moved parallel to the area axis to zero area, it comes into contact with the line of the π–A isotherm of the LS state elongated to the lower surface pressure. The intersection point gives the a^β value. The right-hand side of Eq. 2 is calculated numerically from the π–A curves given in Figs. 4 and 5.

TABLE 1
Apparent Molar Quantity Change on the Phase Transition of FC12 at 298.2 K (0.01 M NaCl, pH 2)

Compound	$-\Delta s^{\gamma}$/(J K^{-1} mol^{-1})	$-\Delta h^{\gamma}$/(kJ mol^{-1})	$-\Delta u^{\gamma}$/(kJ mol^{-1})
FC12	80 (±1)	24 (±1)	41 (±1)
C14 acid[a]	47 (±1)	14 (±1)	17 (±1)

Note. FC12, $a^{c} = 0.284\,\text{nm}^2$, $a^{e} = 0.725\,\text{nm}^2$; C14 acid (tetradecanoic acid), $a^{c} = 0.18\ \text{nm}^2$, $a^{e} = 0.25\ \text{nm}^2$. The above numerical values were used for calculation.

[a] At pH 2. Refs. 28 and 30.

The apparent molar quantity changes (Δs^{γ}, Δh^{γ}, and Δu^{γ}) for FC12 on the phase transition are given in Table 1 together with reference data of a typical fatty acid, tetradecanoic acid (28, 30). As for C12-TAC, the phase transition clearly exists judging from the π–A curves at different temperatures (Fig. 4), but the thermodynamic quantities were not calculated, since the phase of smaller area was not confirmed to be the LS phase by fluorescence microscopy (Fig. 3). The equation used for the energy change is

$$(\Delta u^{\gamma})(\alpha, \beta) = -(\pi^{\text{eq}} - \gamma^{0})(a^{\alpha} - a^{\beta}) + T\,\Delta s^{\gamma}(\alpha, \beta), \quad [3]$$

which corresponds to Eq. 32 of Ref. 28. It can be seen from Table 1 that for the apparent molar enthalpy changes, all the values are negative as expected. That is, the transition from the disordered phase (gaseous or expanded) to the ordered (LS) one is exothermic. The small entropy change of FC12 on the transitions suggests the slightly more constrained state in the monolayer configuration. Apparent molar quantities of FC12 are larger than those of C14 acid. The difference observed in the values of thermodynamics quantities between them clearly evidences the influence of the fluorocarbon chain.

Let us look at the FC12 row in Table 1. The apparent molar entropy change on the transition from the disordered phase (gaseous or expanded) to the ordered (LS) one is -0.8×10^2 J K^{-1} mol^{-1}. On the contrary, that of tetradecanoic acid at pH 2 (28, 30) is 0.58 times that for FC12, although there are minor distinctions caused by dissimilarities in subphase composition. The values of the apparent molar enthalpy change (Δh^{γ}) and of the apparent molar energy change (Δu^{γ}) are of a similar trend. The above result can be expected from a fluorocarbon chain with a carbon number of 6.4. From the bulk properties of many perfluorocarbons the hydropobicity of fluorocarbon was found equal to 1.5-fold those of the same chain length of the hydrocarbon. Our experimental value is, however, about 2-fold instead of 1.5-fold.

3. *Contribution of ω-Group (CF_3) and Polar Head Group to Dipole Moment*

The surface potential of monolayers was often analyzed using the three-layer model proposed by Demchak and Fort (16), as suggested by Davies and Rideal (31). This model postulates independent contributions by the subphase (layer 1), polar head group (layer 2), and hydrophobic chain (layer 3). Independent dipole moments and effective local dielectric constants are attributed to each of the three layers. Other models such as the Helmholtz model and the Vogel and Möbius model (32) are also available. The differences of these models were reviewed in Ref. 33. The conclusion was that, despite its limitations, the Demchak and Fort model provides a good agreement between the values of the dipole moment estimated from the monolayer surface potentials and those determined from measurements on bulk material for various aliphatic compounds.

We have thus compared the experimental values of the vertical components $\mu_{\perp}$ in the closed packed state with the values of $\mu_{\perp\text{calc}}$ calculated from the equation based on the three-layer model:

$$\mu_{\perp\text{calc}} = (\mu_1/\varepsilon_1) + (\mu_2/\varepsilon_2) + (\mu_3/\varepsilon_3), \quad [4]$$

where μ_1/ε_1, μ_2/ε_2, and μ_3/ε_3 are the contributions of the subphase, polar head, and tail-end group, respectively.

The authors wanted to determine the contribution of the terminal CF_3 group and that of the trimethylammonium chloride group. As long as they know, the last has not been determined, yet. However, the conformation of the trimethylammonium chloride group connected with a hydrocarbon chain is likely to be different from that of the group connected with a fluorocarbon chain. In the first approximation, the contributions by three groups were assumed constant and separable. Then, μ_2^{COOH} may be evaluated from the data of stearic acid (C_{18} acid) under the same substrate condition (see Table 2).

$$\mu_{\perp}^{\text{C18}} = \frac{\mu_1}{\varepsilon_1} + \frac{\mu_2^{\text{COOH}}}{\varepsilon_2} + \frac{\mu_3^{\text{CH}_3}}{\varepsilon_3} = 0.18\,\text{D}, \quad [5]$$

The initial set of values proposed by Demchak and Fort ($\mu_1/\varepsilon_1 = 0.040$ D, $\varepsilon_2 = 7.6$, $\varepsilon_3 = 5.3$; Ref. 16) was determined for monolayers of terphenyl derivatives and octadecyl nitrile. Other sets of values were determined from the recent study (25) by Petrov *et al.* ($\mu_1/\varepsilon_1 = 0.040$ D, $\varepsilon_2 = 7.6$, $\varepsilon_3 = 4.2$; and $\mu_1/\varepsilon_1 = 0.025$ D, $\varepsilon_2 = 7.6$, $\varepsilon_3 = 4.2$) and by Taylor and Oliveira ($\mu_1/\varepsilon_1 = -0.065$ D, $\varepsilon_2 = 6.4$, $\varepsilon_3 = 2.8$) for monolayers of

TABLE 2
Surface Potential Data Used for Dipole Moment Evaluation

Compound	A (nm^2)	ΔV (mV)
Stearic acid	0.181 ± 0.001	372 ± 10
FC12	0.250 ± 0.001	−1060 ± 10
C12-TAC	0.340 ± 0.001	333 ± 10

Note. A and ΔV are the values at maximum compression, respectively, where the subphase was 0.01 M NaCl (pH 2) at 298.2 K for the whole compounds.

ω-halogenated fatty acids and amines (33, 34). However, the authors have used the combination of two sets of values ($\mu_1/\varepsilon_1 = -0.065$ D, $\varepsilon_2 = 6.4$, $\varepsilon_3 = 2.8$, and $\mu_3 = 0.33$ D for CH_3 or $\varepsilon_3 = 4.2$ for CF_3), because they provide a good agreement between calculated dipole moments and experimental ones determined for monolayers spread on a saline phase. Some values have been proposed for μ_2 for the different conformations of the COOH (24): μ_2(COOH-α *cis*(*cis*) acid) = 0.820 D, μ_2(COOH-α *trans*(*cis*) acid) = −0.640 D, μ_2(COOH-α *cis*(*trans*) acid) = 3.560 D, μ_2(COOH-α *trans*(*trans*) acid) = 0.990 D, μ_2(COOH-α *cis*(free) acid) = 2.360 D, and μ_2(COOH-α *trans*(free) acid) = 0.250 D. Here, we have used the μ_2(COOH-α *cis*(*cis*) acid) = 0.820 D value, because previous studies support the α *cis*(*cis*) acid conformation for condensed alkyl acid monolayers (16, 35) within the precision of the calculation (ca. 0.010 D).

Assuming the carboxyl moiety to be in the α *cis*(*cis*) acid configuration and using the experimentally determined $\mu_\perp$ values and the above values ($\mu_1/\varepsilon_1 = -0.065$ D, $\varepsilon_2 = 6.4$, $\mu_2 = 0.820$ D, and $\varepsilon_3 = 4.2$), the authors were able to obtain $\mu_3/\varepsilon_3 = -0.763$, or $\mu_3^{CF_3} = -3.2$ D, from Eq. [5]:

$$\mu_\perp^{FC12} = \frac{\mu_1}{\varepsilon_1} + \frac{\mu_2^{COOH}}{\varepsilon_2} + \frac{\mu_3^{CF_3}}{\varepsilon_3} = -0.70\,\text{D}. \qquad [6]$$

This value is a little bit larger compared with those reported for ω-halogenated acid (−1.8–2.2 D) (24) and trifluoropalmitic acid (34) monolayers. This difference may come from experimental conditions such as substrate condition (electrolyte, pH) and compression rates.

Normally, the estimation of a dipole moment of polar head groups and hydrocarbon tail using the Demchak and Fort model holds for un-ionized (condensed) Langmuir monolayers with closely packed vertical chains. Such treatment sets limitations that are not met by the C12-TAC film having a net charge. The problem could be resolved subtracting the Gouy–Chapman potential from the total surface potential as shown by Davis and Rideal (31). This treatment would be much more appropiate for the C12-TAC monolayer. The following equations were employed for the above procedure.

$$\Delta V = \frac{12\pi\mu_D}{A} + \Psi_0 \qquad [7]$$

$$\Psi_0 = \left(\frac{2kT}{ze}\right)\sinh^{-1}\left[\frac{\sigma}{(2\varepsilon\varepsilon_v n_0 kT)^{1/2}}\right] \qquad [8]$$

$$\mu_D = \mu_1 + \mu_2 + \mu_3, \qquad [9]$$

where A refers to area (nm^2), μ_D is the vertical component of the net dipole moment due to the head group of molecules adsorbed at the interface (D), Ψ_0 refers to the electrostatic potential at the interface relative to the adjacent conducting phase (mV), k is the Boltzmann constant, T is the absolute temperature, e is electrostatic unit charge, z is valency of electrolyte, σ is surface charge density (C m^2), ε is dielectric constant (78.3 at 298.2 K), ε_v is vacuum permittivity (8.854×10^{-12} J^{-1} C^2 m^{-1}), and n_0 is the number density of charges in the system. Equation [7] is generalized in order to apply to a charge monolayers; Ψ_0 was calculated to be 0.225 V under the experimental conditions, and then μ_D became 0.097 D. μ_1 cannot be measured, so it is usually combined with μ_2, which means that the reorientation of water dipoles, as expressed by μ_1, may well depend on μ_2.

$$\mu_\perp^{C12TAC} = \frac{\mu_2^{TAC}}{\varepsilon_2} + \frac{\mu_3^{CF_3}}{\varepsilon_3} = 0.097\ \text{D}. \qquad [10]$$

So the value ($\mu_3^{CF_3}/\varepsilon_3$) reported can be inserted into Eq. [10], assuming $\varepsilon_2 = 6.4$ and $\mu_2 = \mu_1 + \mu_2$, which resulted in $\mu_2^{TAC} = 5.5$ D for the trimethylammonium chloride head. A change in ΔV may also result from changes in head group hydration. Comparing −COOH with $-N^+(Me)_3Cl^-$, the value of the dipole moment on $-N^+(Me)_3Cl^-$ is 6.7 times as large as that of −COOH. The contribution of the $-N^+(Me)_3Cl^-$ head group is much larger than that of the fluorinated carbon chain. As a result, the surface potential of C12-TAC shows the positive change, although the number of the carbon atoms of the perfluorocarbon chain is 12.

4. *Ideality of Mixing*

The two-component mixed monolayer system composed of FC12 and C12-TAC was studied in order to assess the effect of the molecular structure of the amphiphiles on their miscibility in the monolayer and on the molecular state of the monolayer. For the above purpose, the π–A, ΔV–A, and $\mu_\perp$–A isotherms of the mixed monolayers of FC12 and C12-TAC were measured for various FC12 molar fractions (X_{FC12}) at 298.2 K on 0.01 M NaCl subsolution and at pH 2.0. The results are shown in Figs. 6a–6d. Between $X_{FC12} = 1.0$ and 0.7, the π–A isotherms display a phase transition pressure that decreases with decreasing X_{FC12}. While between $X_{FC12} = 0.0$ and 0.4 (not shown in Fig. 6), the isotherms also display a transition pressure that decreases with increasing X_{FC12}. Although it is difficult to ascertain the transition pressure between 0.4 and 0.6 mole fractions, the FC12 and C12-TAC mixed systems are, at least, partially miscible in the mixed monolayers.

Figure 6a might suggest that the π–A isotherms can be classified into two types. The first one is for $X_{FC12} = 0$–0.3, and the second one is for $X_{FC12} = 0.3$–1.0. That is, the first type is that all the π–A curves of the mixed systems are between those of the pure components and they successively change with increasing mole fraction of FC12 over the range $X_{FC12} = 0$–0.3. On the other hand, the second type of these curves are rather compressed into a smaller area, showing a smaller molecular area than the π–A isotherm of pure FC12 over the range $X_{FC12} = 0.3$–1. These curves in the expanded scale are shown in Fig. 6d.

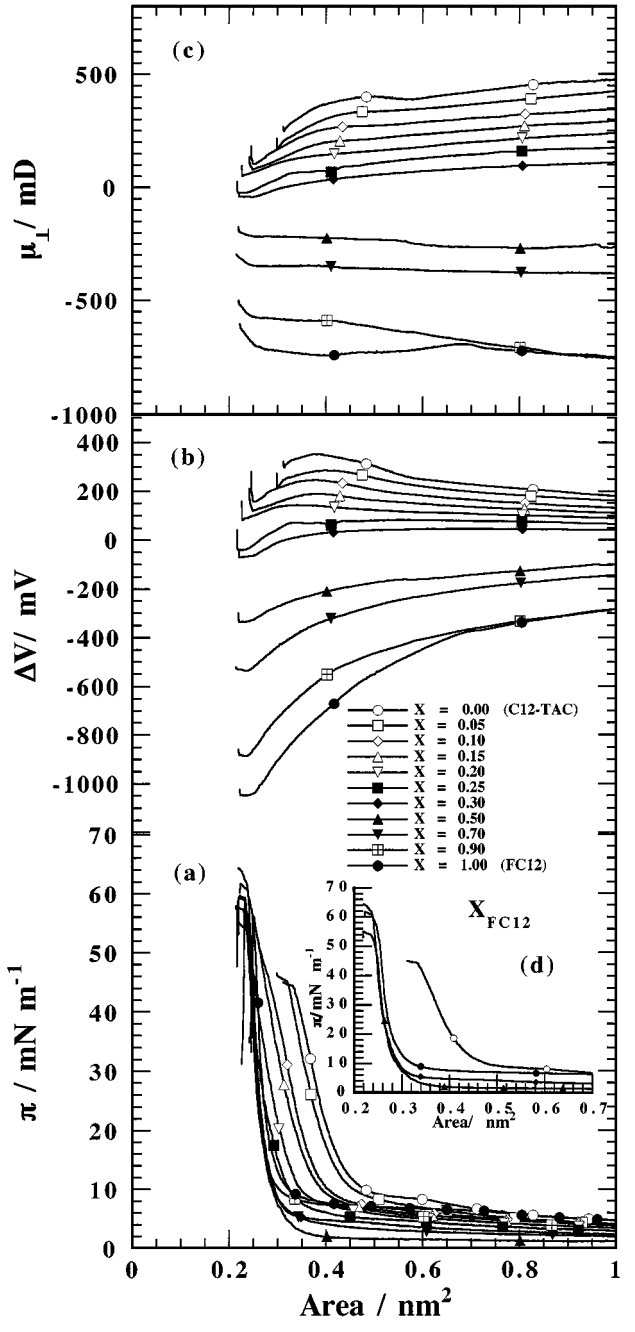

FIG. 6. Surface pressure (π)–area (A) isotherms (a), surface potential (ΔV)–area (A) isotherms (b), surface dipole moment ($\mu_\perp$)–A isotherms (c), and expanded scale (π)–area (A) isotherms (d) of FC12 and C12-TAC mixed monolayers on 0.01 M NaCl (pH 2) at 298.2 K.

In Figs. 6b and 6c the influences of X_{FC12} on the ΔV–A and $\mu_\perp$–A isotherms are also examined. From these figures, the ΔV–A and $\mu_\perp$–A isotherms can be divided into three types. The first type is for $X_{FC12} = 0$–0.2, where the ΔV values exist on the positive side (or $\mu_\perp$). The second type is for the negative side of ΔV (or $\mu_\perp$) over the range $X_{FC12} = 0.5$–1.0. The third, for $X_{FC12} = 0.25$–0.3, is an intermediate type between the first and the second types. That is, ΔV (or $\mu_\perp$) changes from a positive value at a larger area to a negative value at a smaller area, approaching a closely packed area.

The interaction between FC12 and C12-TAC molecules is provided by examining whether the mean molecular areas as a function of X_{FC12} satisfy the additivity rule. Comparison between experimental mean molecular areas (closed circles) and mean molecular areas (dashed lines) of the ideal mixing is shown in Fig. 7 at four pressures (5, 15, 25, and 35 mN m^{-1}). For all pressures, it clearly indicates a negative deviation from the theoretical lines, indicating some excess interactions between FC12 and C12-TAC molecules. These interactions may likely result from attractive interaction between $-N^+(Me)_3Cl^-$ and COOH polar heads.

Figures 6b and 6c examine the influence of the X_{FC12} on the ΔV–A and $\mu_\perp$–A curves. The same analyses of the surface potential (ΔV) and of the surface dipole moment ($\mu_\perp$) of the mixed monolayer were also made in terms of the additivity rule. For the mixed system, the results are presented by solid points

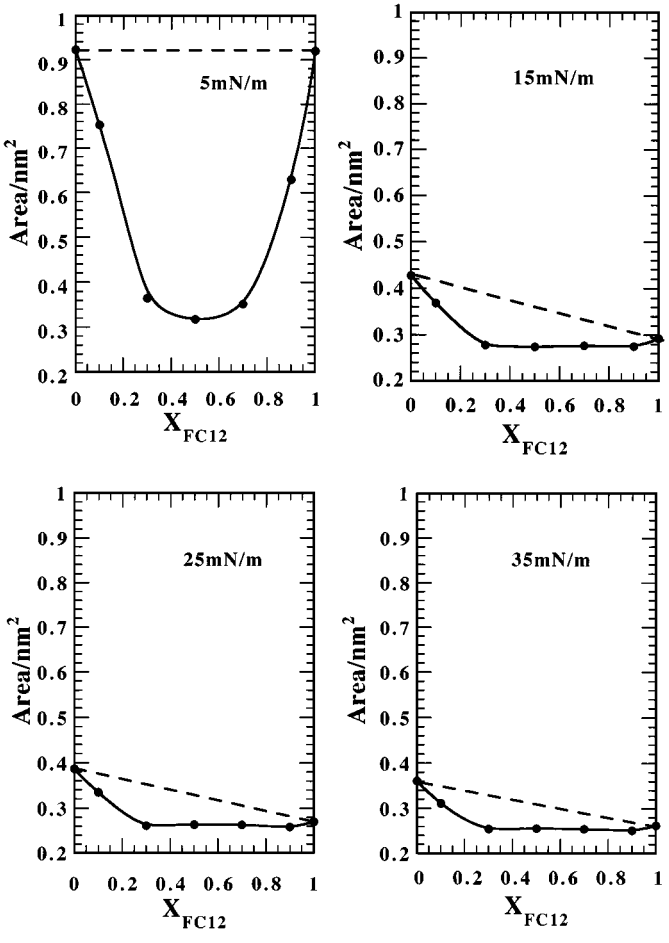

FIG. 7. Mean molecular area (A) of mixed FC12 and C12-TAC system as a function of composition of FC12 at four different pressures. Dashed lines were calculated by assuming the additivity rule; solid circles represent experimental values.

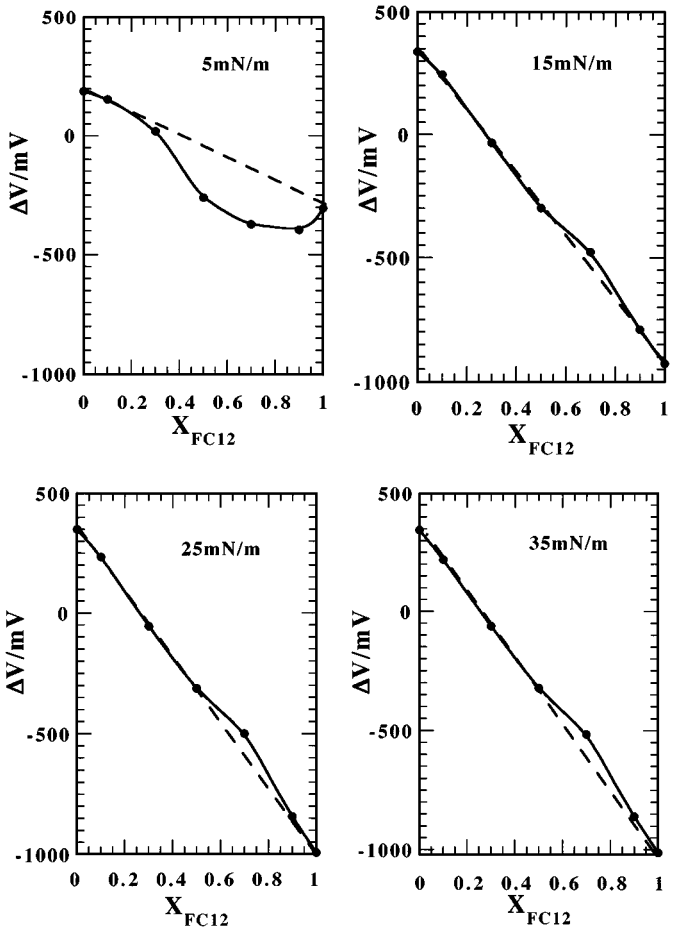

FIG. 8. Surface potential (ΔV) of mixed FC12 and C12-TAC system as a function of composition of FC12 at four different pressures. Dashed lines were calculated by assuming the additivity rule; solid circles represent experimental values.

in Figs. 8 and 9, where the dashed lines are the mean ΔV and the mean $\mu_\perp$ from the additivity rule. The $\mu_\perp$ values at various surface pressures (5, 15, 25, and 35 mN/m) showed a sigmoidal shape, where the deviation from the additivity rule is 100 mD at maximum.

It can be seen from Fig. 6 that the isotherms of $X_{\mathrm{FC12}} =$ 0.3–0.9 on the 0.01 M NaCl electrolyte (pH 2) are compressed to a smaller area than pure FC12 area on the same substrate (Fig. 6d). So there comes the question, what is taking place in the monomolecular state. To investigate the mixed monolayer state of FC12 and C12-TAC, the cospreading method (36–40) was employed for the same system. Typical examples of the mixed monolayer and cospreading of FC12/C12-TAC are shown in Fig. 10. This figure also includes the FC10/C12-TAC system in order to compare it with the FC12/C12-TAC system. FC10 does not form a stable monolayer in the π–A isotherm at 0.01 M NaCl electrolyte (pH 2). The FC10 system shows a big difference in the π–A, ΔV–A, and $\mu_\perp$–A isotherms from the FC12 and C12-TAC system. At the same time, FC10 and FC12 have a different initial pressure. However, as for the mixed monolayer, the monolayer formed by cospreading of FC10 and C12-TAC, there is little difference between the two systems in the π–A, ΔV–A, and $\mu_\perp$–A isotherms, except for a small difference in the collapse pressure. This is also the case for the FC12 and C12-TAC mixed monolayer and for the FC12 and C12-TAC cospreading systems, and, therefore, the π–A, ΔV–A, and $\mu_\perp$–A isotherms are completely the same. The FC12 and C12-TAC are approximately the same in chain length, and a cohesive force between their fluorocarbon chains is stronger than that for the FC10 and C12-TAC system. The π–A isotherm of the FC12 and C12-TAC system is shifted to a smaller area compared with that of the FC10 and C12-TAC system. The difference in cohesive force between the mixed systems is reflected upon the ΔV–A and $\mu_\perp$–A isotherms' behaviors. Judging from the above observation, it is quite clear that the outstanding condensing effect on the π–A isotherms results from the complex formation by strong ionic interaction between the head groups. The complex formation of a one–one ratio in a bulk solid was also confirmed by elemental analysis.

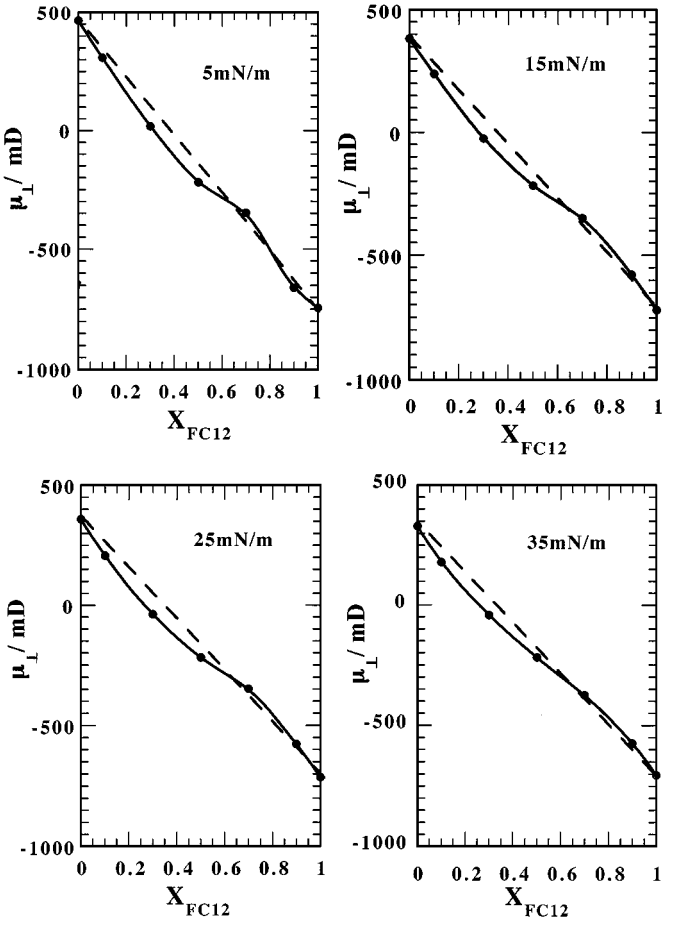

FIG. 9. Surface dipole moment ($\mu_\perp$) of mixed FC12 and C12-TAC system as a function of composition of FC12 at four different pressures. Dashed lines were calculated by assuming the additivity rule; solid circles represent experimental values.

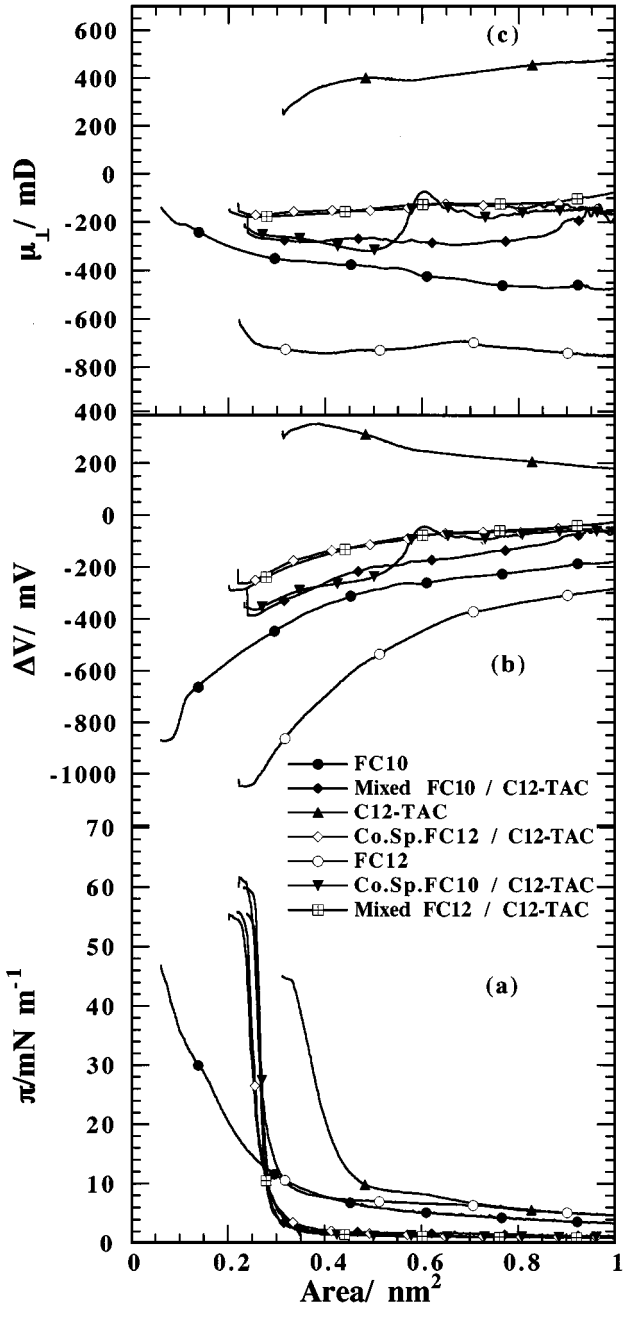

FIG. 10. Surface pressure (π)–area (A) isotherms (a), surface potential (ΔV)–area (A) isotherms (b), and surface dipole moment ($\mu_\perp$)–A isotherms (c) of mixed FC12 and C12-TAC system and cospreading FC12 and C12-TAC system on 0.01 M NaCl (pH 2) at 298.2 K. Mixed, mixed monolayer is composed of FC12 and C12-TAC; Co-s, cospreading FC12 and C12-TAC.

5. *Two-Dimentional Phase Diagram*

A two-dimentional phase diagram of the FC12/C12-TAC monolayer is shown in Fig. 11. Filled circles are the collapse pressure π^c determined at different mole fractions, while the dashed line is the collapse pressure for $\xi = 0$ from Eq. [11]. The coexistence phase boundary between the expanded and the bulk phases of the FC12/C12-TAC mixture can be theoretically simulated by the Joos equation (17)

$$1 = x_1^s \gamma_1 \exp\left(\frac{\pi_{c,m} - \pi_{c,1}}{kT}\omega_1\right) \exp\left[\xi\left(x_2^s\right)^2\right] + x_2^s \gamma_2 \exp\left(\frac{\pi_{c,m} - \pi_{c,2}}{kT}\omega_2\right) \exp\left[\xi\left(x_1^s\right)^2\right], \quad [11]$$

where x_1^s and x_2^s denote the mole fraction at the surface of components 1 and 2; $\pi_{c,1}$ and $\pi_{c,2}$ are the corresponding collapse pressures; $\pi_{c,m}$ is the collapse pressure of the mixed monolayer at given compositions of the surface, x_1^s and x_2^s; ω_1 and ω_2 are limiting areas at the collapse point; γ_1 and γ_2 are the surface activity coefficients at the collapse point; ξ is the interaction parameter; and kT is the product of the Boltzmann constant and the Kelvin temperature. The solid curve is made coincide with the experimental values by adjusting the interaction parameter ξ of the above equation. Here it is noteworthy that the FC12/C12-TAC system produces a negative interaction parameter. The new finding is that the FC12/C12-TAC mixed system has two interaction parameters; $\xi = -4.20$ for $X_{FC12} = 0$–0.5, and $\xi = -0.24$ for $X_{FC12} = 0.5$–1. So, the two regions in the two-dimensional phase diagram result. The first region is $X_{FC12} = 0$–0.5, where FC12 and C12-TAC components form a certain complex. That is, this region consists of the complex and excess C12-TAC, where the FC12/C12-TAC complex grows until X_{FC12} becomes 0.5. The second region consists of the FC12/C12-TAC complex and excess FC12. The negative interaction parameter implies that the interchange energy between the two molecules is larger than the mean of interaction energies between the same molecules. And the interaction energies ($\Delta\varepsilon$) were calculated to be 1.74 kJ/mol

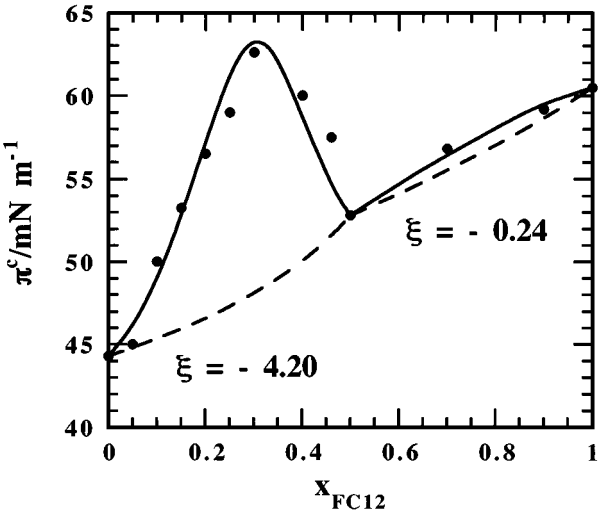

FIG. 11. Collapse presssure (π^c) as a function of the surface composition of FC12 in a mixed monolayer. The solid was line calculated according to Eq. [11]; the dashed line was calculated according to Eq. [11] in the case of $\xi = 0$. Solid circles represent experimental values.

($\xi = -4.20$) and 99 J/mol ($\xi = -0.24$). Thus, the two components are miscible in the expanded state as well as in the condensed state. Their mutual interaction energy between the two components in the mixed monolayer is stronger than the mean of the interaction energies, as mentioned above (Refs. 18a–18d). Figure 9 ($\mu_\perp - X_{FC12}$ relationship) shows common characteristics of mixed monolayers in which ion–ion or ion–dipole interaction takes place. The surface potential must result in a negative deviation from the additivity rule, since ion–ion or ion–dipole interaction reduces the average surface dipole per molecule in the mixed monolayer (41, 42). To investigate the above phenomena in more detail, the miscibility of the FC12/C12-TAC system must be further studied by other techniques such as ellipsometry, Brewster angle microscopy, and fluorescence microscopy, which will be reported in a future paper.

In conclusion, the new finding of this study is that single-chain C12-TAC can be spread as a stable monolayer at 298.2 K on 0.01 M NaCl subphase at pH 2 and that C12-TAC exhibits a certain phase transition. The two polar heads, the trimethylammonium chloride group and the carboxyl group, strongly influenced the surface potentials. The Demchak and Fort model and the Gouy–Chapman equation were applied to analyse the surface potentials of FC12 and C12-TAC, respectively, from which the dipole moments of the head group (trimethylammonium chloride) and of the terminal group (CF_3) were determined. Then, it was found that the hydrophilic head groups contribute significantly to the surface potential. The outstanding condensing effect on the $\pi - A$ isotherms ($X_{FC12} \geq 0.3$) may result from the complex formation. Assuming a regular surface mixture, the Joos equation was applied to trace the collapse pressure of a mixed monolayer for miscible components. The two regions in the two-dimensional diagram were proposed, where the interaction parameters evaluated ($\xi = -4.20$, and -0.24, i.e., an interchange energy of 1.74 kJ mol^{-1} and 99 J mol^{-1}, respectively) indicate miscibility of the fluorinated amphiphiles in a monolayer state.

ACKNOWLEDGMENTS

This work was supported by Grant-in-Aid for Scientific Research No. 10554040 from the Ministry of Education, Science and Culture, Japan; this support is greatly appreciated. We also thank Professor M. Kawaguchi (Mie University, Japan) for helpful and stimulating discussions about fluorescence images.

REFERENCES

1. Kissa, E., *in* "Fluorinated Surfactants: Synthesis, Properties, Applications." Dekker, New York, 1994.
2. Riess, J. G., *Colloids Surf.* **84,** 33–48 (1994); Krafft, M. P., and Riess, J. G., *Biochemie* **80,** 489–514 (1998); Riess, J. G., and Krafft, M. P., *Biomaterials* **19,** 1529–1539 (1998).
3. Krafft, M. P., Riess, J. G., and Weers, J. G., *in* "Submicronic Emulsions in Drug Targeting and Delivery" (S. Benita, Ed.), chap. 10, pp. 235–333. Harwood Academic, Amsterdam, 1998; Sadtler, V. M., Krafft, M. P., and Riess, J. G., *Angew. Chem. Int. Ed. Engl.* **35,** 1976–1978 (1996).
4. Riess, J. G., *J. Drug Target.* **2,** 455–468 (1994); Riess, J. G., and Krafft, M. P., *Chem. Phys. Lipids* **75,** 1–14 (1995); Krafft, M. P., Giulieri, F., and Riess, J. G., *Angew. Chem. Intl. Ed. Engl.* **332,** 741–743 (1993); Riess, J. G., Frézard, F., Greiner, J., Krafft, M. P., Santaella, C., Vierling, P., and Zarif, L., *in* "Liposomes—Non-medical Applications" (Y. Barenholz and D. Lasic, Eds.), Vol. III, p. 97. CRC Press, Boca Raton, FL, 1996.
5. Giulieri, F., Krafft, M. P., and Riess, J. G., *Angew. Chem. Intl. Ed. Engl.* **34,** 1514–1515 (1996); Giulieri, F., Guillot, F., Greiner, J., Krafft, M. P., and Riess, J. G., *Chem. Eur. J.* **2,** 1335–1339 (1996).
6. Riess, J. G., *in* "Blood Substitutes: Principles, Methods, Products and Clinical Trials" (T. M. S. Chang, Ed.), pp. 101–126. Karger Landes Systems, Georgetown, 1999; Riess, J. G., *New J. Chem.* **19,** 893 (1995); Riess, J. G., *Art. Cells Blood Subst. Immob. Biotech.* **22,** 123–360 (1994).
7. Adamson, N. K., *in* "The Physics and Chemistry of Surfaces," Chap. 2. Dover, New York, 1968.
8. Harkins, W. D., *in* "The Physical Chemistry of Surface Films," Chap. 2. Reinhold, New York, 1952.
9. Gaines, G. L., *in* "Insoluble Monolayer at Liquid–Gas Interface." Interscience, New York, 1966.
10. (a) Matuo, H., Yoshida, N., Motomura, K., and Matuura, R., *Bull. Chem. Soc. Jpn.* **52,** 667 (1979); (b) Matuo, H., Motomura, K., and Matuura, R., *Bull. Chem. Soc. Jpn.* **52,** 663 (1979), and **54,** 2205, (1981); (c) Matuo, H., Motomura, K., and Matuura, R., *Chem. Phys. Lipids* **28,** 281–385 (1981) and **30,** 353, (1982); (d) Matuo, H., Rice, D. K., Balthasar, D. M., and Cadenhead, D. A., *Chem. Phys. Lipids* **30,** 367 (1982); (e) Matuo, H., Mitsui, T., Motomura, K., and Matuura, R., *Chem. Phys. Lipids* **29,** 55 (1981).
11. Yamamoto, S., Shibata, O., Lee, S., and Sugihara, G., *Prog. Anesthesiol. Mech.* **3** (Special Issue), 25–30 (1995).
12. Shibata, O., Yamamoto, S., Lee, S., and Sugihara, G., *J. Colloid Interface Sci.* **184,** 201 (1996).
13. Krafft, M. P., Giulieri, F., Huo, Q., and Leblance, R. M., in preparation.
14. Wang, S., Lunn, R., Krafft, M. P., and Leblance, R. M., *Langmuir* **16,** 2882–2886 (2000).
15. Yamabe, T., Moroi, Y., Abe, Y., and Takahashi, T., *Langmiur* **16**(25), 9754–9758 (2000).
16. Demchak, R. J., and Fort, T., Jr., *J. Colloid Interface Sci.* **46,** 191–202 (1974).
17. Joos, P., and Demel, R. A., *Biochim. Biophys. Acta* **183,** 447 (1969).
18. (a) Shibata, O., Moroi, Y., Saito, M., and Matuura, R., *Langmiur* **8,** 1806 (1992); (b) Shibata, O., Moroi, Y., Saito, M., and Matuura, R., *Thin Solid Films* **242,** 273 (1994); (c) Shibata, O., Miyoshi, H., Nagadome, S., Sugihara, G., and Igimi, H., *J. Colloid Interface Sci.* **146,** 595 (1991); (d) Miyoshi, H., Nagadome, S., Sugihara, G., Kagimoto, H., Ikawa, Y., Igimi, H., and Shibata, O., *J. Colloid Interface Sci.* **149,** 216 (1992); (e) Shibata, O., Moroi, Y., Saito, M., and Matuura, R., *Thin Solid Films* 327–329, 123 (1998).
19. Acero, A. A., Li, M., Lin, B., Rice, S. A., Goldmann, M., Azouz, I. B., Goudot, A., and Rondelez, F., *J. Chem. Phys.* **99**(9), 7214–7220 (1993).
20. Shin, S., and Rice, S. A., *Langmuir* **10,** 262 (1994).
21. Shin, S., and Rice, S. A., *J. Chem. Phys.* **101**(3), 2508 (1994).
22. Fox, H. W., *J. Phys. Chem.* **61,** 1058 (1957).
23. Bernett, M. K., and Zisman, W. A., *J. Phys. Chem.* **67,** 1534–1540 (1963).
24. Bernett, M. K., Jarvis, N. L., and Zisman, W. A., *J. Phys. Chem.* **68,** 3520–3529 (1964).
25. Petrov, J. G., Polymeropoulos, E. E, and Möhwald, H., *J. Phys. Chem.* **100,** 9860–9868 (1996).
26. Shibata, O., Kaneshima, S., Nakamura, M., and Matuura, R., *J. Colloid Interface Sci.* **95,** 87 (1983).
27. Shibata, O., *J. Colloid Interface Sci.* **96,** 182 (1983).
28. Motomura, K., Yano, T., Ikematsu, M., Matuo, H., and Matuura, R., *J. Colloid Interface Sci.* **69,** 209 (1979).
29. Jones, G. L., and Ray, W. A., *J. Am. Chem. Soc.* **63,** 3262 (1941); Shaw, D. J., *in* "Introduction to Colloid and Surface Chemistry," p.78. Butterworth, London, 1989.

30. Motomura, K., Ikematsu, Hayami, Y. M., Matuo, H., and Matuura, R., *Bull. Chem. Soc. Jpn.* **53,** 2217 (1980).
31. Davies, J. T., and Rideal, E. K., *in* "Interfacial Phenomena," 2nd ed., p. 71. Academic Press, New York, 1963.
32. Vogel, V., and Möbius, D., *J. Colloid Interface Sci*. **126,** 408–420 (1988); Vogel, V., and Möbius, D., *Thin Solid Films* **159,** 73 (1988).
33. Taylor, D. M., Oliveira, O. N., Jr., and Morgan, H., *J. Colloid Interface Sci*. **139,** 508–518 (1990); Morgan, H., Taylor, D. M., and Oliveira, O. N., Jr., *Biochim. Biophys. Acta* **1062,** 149 (1991).
34. Oliveira, O. N., Jr., Riul, A., and Leal Ferreira, G. F., *Thin Solid Films* **242,** 239–242 (1994).
35. Oliveira, O. N., Jr., Taylor, D. M., Lewis, T. J., Salvago, S., and Stirling, J. M., *J. Chem. Soc. Faraday Trans. 1* **85,** 1009 (1989).
36. Hada, H., Hanawa, R., Haraguchi, A., and Yonezawa, Y., *J. Phys. Chem*. **89,** 560 (1985).
37. Yonezawa, Y., Möbius, D., and Kuhn, H., *Ber. Bunsenges. Phys. Chem*. **90,** 1183 (1986).
38. Cordroch, W., and Möbius, D., *Thin Solid Films* **210/211,** 135 (1992).
39. Schoeler, U., Tews, K. H., and Kuhn, H., *J. Chem. Phys.* **61,** 5009 (1974).
40. Martín, M. T., Prieto, I., Camacho, L., and Möbius, D., *Langmuir* **12,** 6554 (1996).
41. Marsden, J., and Schulman, J. H., *Trans. Faraday. Soc*. **34,** 748 (1938).
42. Shah, D. O., and Schulman, J. H., *J. Lipid Res.* **6,** 341 (1965).